ELSEVIER

Physica A 277 (2000) 359–388

PHYSICA A

www.elsevier.com/locate/physa

Intermittency exponents and energy spectrum of the Burgers and KPZ equations with correlated noise

Mahendra K. Verma

Department of Physics, Indian Institute of Technology, Kanpur – 208016, India

Received 1 October 1999

Abstract

We numerically calculate the energy spectrum, intermittency exponents, and probability density $P(u')$ of the one-dimensional Burgers and KPZ equations with correlated noise. We have used pseudo-spectral method for our analysis. When σ of the noise variance of the Burgers equation (variance $\propto k^{-2\sigma}$) exceeds 3/2, large shocks appear in the velocity profile leading to $\langle|u(k)|^2\rangle \propto k^{-2}$, and structure function $\langle|u(x+r,t)-u(x,t)|^q\rangle \propto r$ suggesting that the Burgers equation is intermittent for this range of σ. For $-1\leqslant\sigma\leqslant 0$, the profile is dominated by noise, and the spectrum $\langle|h(k)|^2\rangle$ of the corresponding KPZ equation is in close agreement with the Medina et al. renormalization group predictions. In the intermediate range $0<\sigma<3/2$, both noise and well-developed shocks are seen, consequently the exponents slowly vary from RG regime to a shock-dominated regime. The probability density $P(h)$ and $P(u)$ are Gaussian for all σ, while $P(u')$ is Gaussian for $\sigma=-1$, but steadily becomes non-Gaussian for larger σ; for negative u', $P(u')\propto\exp(-ax)$ for $\sigma=0$, and approximately $\propto u'^{-5/2}$ for $\sigma>1/2$. We have also calculated the energy cascade rates for all σ and found a constant flux for all $\sigma\geqslant 1/2$.

PACS: 47.27.Cn; 47.54.+r; 68.10.−m; 02.50.Ey

1. Introduction

Stochastic Burgers equation has been studied extensively because of its close connection with the Navier–Stokes equation. Recently it has been found that Burgers equation with correlated noise shows intermittency [1–3], however, these calculations have been done for specific degrees of noise correlation. In this paper we vary the applied noise

E-mail address: mkv@iitk.ac.in (M.K. Verma)

0378-4371/00/$ - see front matter
PII: S0378-4371(99)00544-0

from uncorrelated regime to strongly correlated regime and study the energy spectrum of h and u, as well as intermittency exponents and the probability densities of u and $\mathrm{d}u/\mathrm{d}x$, where $u(x,t)$ is the velocity function appearing in the Burgers equation, and $h(x,t)$ is the surface height of KPZ equation.

The one-dimensional Burgers equation [4] is

$$\frac{\partial u}{\partial t} + \lambda u \frac{\partial u}{\partial x} = \nu \frac{\partial^2 u}{\partial x^2} + \zeta\,, \tag{1.1}$$

where u is the velocity field, λ is the strength of the nonlinear term ($\lambda = 1$ in the standard equation), ν is the viscosity, and ζ is the noise. We assume that the noise $\zeta(k,t)$ is Gaussian ($\zeta(k)$ is the Fourier transform of $\zeta(x)$), and in Fourier space follows the distribution

$$\langle \zeta(k,t)\zeta(k',t')\rangle = 2Dk^{-2\sigma}(2\pi)^2\delta(k+k')\delta(t-t')\,. \tag{1.2}$$

Tatsumi and Kida [5], Kida [6], Gotoh [7], and Bouchaud et al. [8] have solved the noiseless Burgers equation ($\zeta = 0$) exactly in limit of large time t and zero viscosity. The solution is a linear profile with sharp discontinuities, which are called shocks. This shock solution yields structure function $\langle |u(x+r,t) - u(x,t)|^q\rangle \propto r$ indicating that the u is intermittent. The solution also yields the energy spectrum $\langle |u(k)|^2/2\rangle \propto k^{-2}$ ($u(k)$ is the Fourier transform of $u(x)$).

The noisy Burgers equation as well as the noisy Kardar–Parisi–Zhang (KPZ) equation have been studied by many authors. The Kardar–Parisi–Zhang (KPZ) equation, which describes a generic set of surface growth phenomena, is closely related to the Burgers equation. The replacement of u by $-\partial h/\partial x$ in the Burgers equation yields KPZ equation

$$\frac{\partial h}{\partial t} = \frac{\lambda}{2}\left(\frac{\partial h}{\partial x}\right)^2 + \nu\frac{\partial^2 h}{\partial x^2} + f(\mathbf{x},t)\,, \tag{1.3}$$

where $h(x,t)$ is the height of the surface profile at position x and at time t, λ is the strength of the nonlinearity, ν is the diffusion coefficient, and f is the forcing function. We again assume that the noise $f(k,t)$ is Gaussian, and in Fourier space follows the distribution

$$\langle f(k,t)f(k',t')\rangle = 2Dk^{-2\rho}(2\pi)^2\delta(k+k')\delta(t-t')\,. \tag{1.4}$$

It is easy to see that $|u(k)|^2 = k^2|h(k)|^2$ and $\sigma = \rho - 1$. In the following several paragraphs we will describe the work done by various researchers regarding energy spectrum, intermittency exponents, and probability densities of h and u when noise is present in the system.

Eq. (1.3) has been solved by Kardar–Parisi–Zhang [9] for $\sigma = -1$ and by Medina et al. [10] for $-1 < \sigma \leqslant 0$ using renormalization group analysis. They have calculated the roughening exponents χ_{KPZ} and β_{KPZ}, which characterize the dynamical properties of the equation, e.g., $\langle |h(k)|^2\rangle \propto k^{-2\chi_{\mathrm{KPZ}}-1}$. The RG analysis is not applicable beyond $\sigma = 0$. Using the connection of the Burgers equation with the KPZ equation, the dynamical exponents of the Burgers equation is also automatically solved for this set of σ.

Recently, Chattopadhyay and Bhattacharjee [11] have applied mode coupling scheme and obtained the same exponents for KPZ equation for $-1 \leqslant \sigma \leqslant 0$.

For $\sigma = -1$, Barabasi and Stanley [12] have shown that in 1D KPZ equation, the function $\mathrm{d}h/\mathrm{d}x(=-u)$ has a Gaussian probability density under steady state. Since h' is Gaussian, we can immediately determine the structure function $T_q(r) = \langle |h(x+r) - h(x)|^q \rangle$ using the following arguments. Since $\Delta h \approx rh'$ for small r, $\Delta h[=h(x+r)-h(x)]$ will also have a Gaussian probability density, i.e.,

$$P(\Delta h) = \frac{1}{\sigma_r \sqrt{\pi}} \exp\left(-\frac{(\Delta h)^2}{\sigma_r^2} \right) . \tag{1.5}$$

Therefore,

$$\langle |\Delta h|^q \rangle = \int_{-\infty}^{\infty} P(\Delta h) |\Delta h|^q \, \mathrm{d}\Delta h \, .$$

$$\propto \sigma_r^q \, . \tag{1.6}$$

In the region where $\langle |\Delta h|^q \rangle$ is a power law (region of our interest), σ_r will also be a power law, say, $\sigma_r \propto r^\chi$. Therefore, $\langle |\Delta h|^q \rangle \propto r^{\chi q}$.

The above discussion clearly shows that if the derivative of the function has a Gaussian probability density, then the exponent of the qth-order structure function (denoted by ζ_q) is proportional to q. These kind of functions are called *non-intermittent* functions. On the other hand, if the probability density of the derivative is non-Gaussian, or the exponent of qth-order structure function is not proportional to q, then the function is said to be *intermittent*. The intermittent functions have typically power-law tails instead of Gaussian tails in their probability densities, hence, probability of occurrence of large value of the function is higher for the intermittent functions then the non-intermittent functions. In other words, large events, which are absent in non-intermittent systems, occur in intermittent systems in a bursty manner. In fluid turbulence, it has been found that $P(u)$ is Gaussian, whereas $P(u'_L)$ and $P(u'_T)$ (where L and T denote longitudinal and transverse components) have power law tails for small r. The exponents of the structure functions are not proportional to q either. Hence, fluid turbulence is said to have intermittency. These observations are explained using localized vortices. For further discussions on intermittency in fluid turbulence, refer to Frisch [13] and references therein.

Chekhlov and Yakhot [1], and Hayot and Jayaprakash [3] numerically solved the structure function of the Burgers equation with correlated noise for a range of σ. For $\sigma = 1/2$, Chekhlov and Yakhot [1] obtained $\langle |\Delta u(r)|^q \rangle \propto r$ and claimed that the Burgers equation is intermittent according to the above definitions. Hayot and Jayprakash [3] found similar results for $0 \leqslant \sigma \leqslant 1/2$. This behaviour was attributed to the shocks present in the system [1,3].

Regarding the energy spectrum, Chekhlov and Yakhot [1] obtained Kolmogorov's energy spectrum, i.e., $|u(k)|^2 \propto k^{-5/3}$ for $\sigma = 1/2$. They argued the constancy of energy flux to be the reason for Kolmogorov's spectrum in the noisy Burgers equation with $\sigma = 1/2$. In this paper we will show that energy flux is constant for all $\sigma \geqslant 1/2$, yet the

spectral exponent varies from 5/3 to 2. Hence, Chekhlov and Yakhot [1] claim that the constancy of flux implies Kolmogorov's spectrum for Burgers equation is incomplete.

Hayot and Jayaprakash [3] have numerically calculated the energy spectrum for $-1 \leqslant \sigma \leqslant 1/2$. For $-1 \leqslant \sigma$, they observed that at large k the behaviour is that of free field, and at low k is in agreement with the result derived using RG treatment. In our simulation we do not find any such crossover. For $0 \leqslant \sigma \leqslant 1/2$, Hayot and Jayaprakash argue that the shocks determine the exponents; their numerical exponent for energy is quite close to the renormalization group formula even though RG is not expected to work in this regime. They also find that the exponent $\beta_{\mathrm{Burg}} = 1/2$ for the Burgers equation.

Polyakov [2] has applied methods of quantum field theory to calculate probability density $P(u')$ of the Burgers equation with $\sigma \geqslant 3/2$, and showed that

$$P(u') = \begin{cases} \exp[-u'^3/(3B_1)] & \text{if } u' \to \infty\,, \\ u'^{-5/2} & \text{if } u' \to -\infty\,. \end{cases} \tag{1.7}$$

Clearly, the probability density of u' is non-Gaussian and has a power-law tail for negative u'. Boldyrev [14,15] extended Polyakov's method to the range $1/2 \leqslant \sigma \leqslant 3/2$ and calculated $P(u')$. He derived that $\chi = 1 + 2\sigma/3$ for $1/2 \leqslant \sigma \leqslant 3/4$, and $\chi = 3/2$ for $\sigma > 3/4$. Boldyrev [14] suggests that the above formula may also be valid for $0 \leqslant \sigma \leqslant 3/2$.

Gotoh and Kraichnan [16] found the exponent of $P(u')$ for the negative u' to be -3. Recently, E and Eijnden [17] and Kraichnan [18] argue the exponent to be $-7/2$. Gurarie and Migdal [19], and Balkovsky et al. [20] have applied instanton solutions for solving probability density for positive u' and obtained qualitative agreement with the numerical results reported by Yakhot and Cheklov [21]. In this paper we will compare our findings with the above-mentioned results.

The roughening exponents for KPZ equation χ_{KPZ} and β_{KPZ} have also been calculated by Zhang by replica method [22], and by Hentschel and Family using scaling arguments [23]. They find a close agreement with the results of Medina et al. [10]. Numerically, Peng et al. [24] have calculated the exponents χ_{KPZ} and β_{KPZ} using finite-difference method, and Amar et al. [25] and Meakin and Jullien [26,27] have calculated using lattice simulations. Their results are in qualitative agreement with the RG predictions.

The energy cascade rate is one of the important quantities of interest in the statistical theory of turbulence. In this paper we have computed the energy flux of the Burgers equation for $-1 \leqslant \sigma < 6$. We find a constant flux for all σ beyond 1/2. In our simulation we also varied the values of the parameters (ν, λ, D) and analysed its effects. We find that there are interesting crossover from KPZ to Edward Wilkinson (EW) equation depending on the values of the parameter. These crossover results are reported in Appendix A.

The outline of the paper is as follows: We restate the structure function and $P(u')$ of the noiseless Burgers and KPZ equations in Section 2, and the energy spectrum of these equations in Section 3. From the nature of the noise–noise correlation, we divide

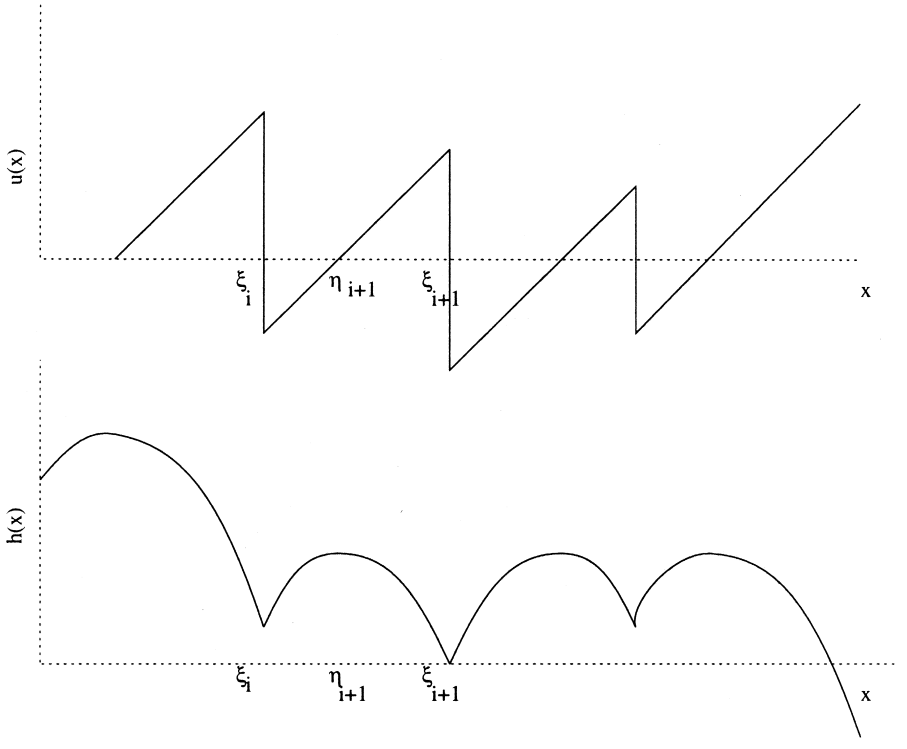

Fig. 1. The solutions of noiseless Burgers and KPZ equations.

the σ regime in three parts. This result is discussed in Section 4. Sections 5 and 6 contain the simulation method and results respectively. Here we calculate the energy spectrum and structure functions of the Burgers and KPZ equations for various values of σ. The probability densities of u' and u are also discussed in this section. Section 7 contains a brief discussion on the cascade rate of the noisy Burgers equation. Section 8 contains discussion and conclusions.

2. Structure function calculation for noiseless case

We will show later that the Burgers equation with strongly correlated noise has behaviour similar to the noiseless Burgers equation. Therefore, we will discuss the noiseless equation briefly before embarking on the noisy Burgers equation. Burgers [4] solved the Burgers equation exactly at large time t for vanishing viscosity. The velocity profile at a given time is linear except for the sharp discontinuities at the shock positions (see Fig. 1). The structure function of the noiseless Burgers equation $S_q(r)$ has been calculated using this solution (see Gotoh [7], Bouchaud et al. [8] and others). Assuming the ensemble average to be the same as the spatial average, Gotoh

obtained

$$S_q(r) = \frac{1}{L}\int_0^L |u(x+r)-u(x)|^q \,\mathrm{d}x$$
$$= \frac{1}{L}\sum_i \int_{\xi_i}^{\xi_{i+1}-r} \left(\frac{r}{t}\right)^q \mathrm{d}x + \frac{1}{L}\int_{\xi_{i+1}-r}^{\xi_{i+1}} \left(\mu_{i+1}-\frac{r}{t}\right)^q \mathrm{d}x$$
$$\approx \left(\frac{r}{t}\right)^q + \frac{r}{L}\sum_i \left(\mu_i - \frac{r}{t}\right)^q , \qquad (2.1)$$

where L is the length of the box, μ_i is the shock strength (defined as the velocity difference across the shock) of the ith shock, and ξ_i is the position of the ith shock. The second term of the equation is due to the discontinuities at the shocks. For small r and $q > 1$, the second term will dominate the first one. Hence, for small r, $S_q(r) \propto r^{\zeta_q^{\mathrm{Burg}}}$ with

$$\zeta_q^{\mathrm{Burg}} = 1 . \qquad (2.2)$$

Note that this relationship is valid for $\delta \ll r \ll \Delta$, where δ is the shock width, and Δ is the average distance between two shocks. For $\nu \to 0$, δ is finite but small (for details, see Saffman [28]). Since u is continuous within the shock, $S_q(r) = r^q$ for $r \ll \delta$. For large r, $S_q(r)$ is not proportional to r because of the $(\mu_i - r/t)^q$ term of Eq. (2.1).

A point is in order here. Tatsumi and Kida [5] showed that the number of shock fronts decrease with t as $t^{-\gamma}$, where $0 \leqslant \gamma < 1$. Hence in the asymptotic state, there will be only several shocks, and the distance between the shock fronts will be of the order of box size. Therefore, asymptotically Δ will be of the order of the box size L, and r can be comparable to L.

As mentioned in the introduction, the structure function is closely related to intermittency. Since the exponent ζ_q^{Burg} is not proportional to q, the noiseless Burgers equation is classified as intermittent system. However, a point to note is that the velocity of the noiseless Burgers equation is not random. From the velocity profile it is clear that $P(u) = const$ for u between $u_{\min}$ and $u_{\max}$. The slope u' is a constant (c) for all u except within the shock region where u' is large but negative. Therefore, $P(u')$ will be a sum of a delta function at $u' = c$ and a small spiky function at large but negative u' (see Fig. 2). Since u is not random, it is somewhat confusing to call the signal as intermittent. However, it is common practice to classify the noiseless Burgers equation as an intermittent system.

For fluid turbulence it has been shown that the intermittent velocity field has a multi-fractal distribution. This was demonstrated by Meneveau and Srinivasan [29,30] using the cascade model. We will apply the same model to Burgers turbulence for a further understanding of the intermittent nature of the Burgers solution.

In the cascade model of Meneveau and Sreenivasan [29,30] for fluid turbulence, the nonlinear energy flux E_r is distributed unequally between two smaller eddies. The flux E_r at length scale r is divided into fractions $p_1 E_r$ and $p_2 E_r$ to two smaller eddies

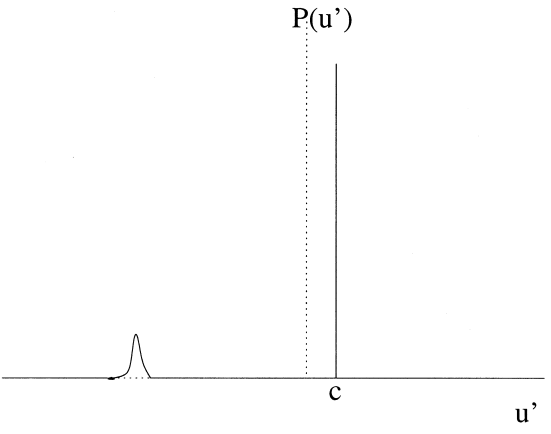

Fig. 2. The probability density $P(u')$ vs. $u'/u'_{\max}$ for the noiseless Burgers equation.

of length $r/2$, and so on. The generalized dimension of the resulting multifractal is given by

$$D_q = \log_2\{p_1^q + p_2^q\}^{1/(1-q)} . \tag{2.3}$$

The constants D_q are related to the exponents of the structure function of the energy flux E_r^q in eddy of size r by

$$\sum E_r^q = E_L^q \left(\frac{r}{L}\right)^{(q-1)D_q} , \tag{2.4}$$

where the sum is taken over all the eddies at the nth stage. When $p_1 \neq p_2$, the flux function is unevenly distributed after several bifurcations of the original eddy, and that yields bursty behaviour for E_r. A closer inspection shows that the Burgers solution corresponds to $p_1 \to 0$ and $p_2 \to 1$, which implies that $D_q \approx 0$. Hence, for Burgers turbulence, only one among the 2^n eddies has all the flux after n bifurcation of the original eddy. This corresponds to maximal intermittency or maximal multiscaling. Using Eq. (5.6) of Meneveau and Sreenivasan [30], we get

$$\zeta_q^{\text{Burg}} = (q/3 - 1)D_q + 1 = 1 , \tag{2.5}$$

a result consistent with Eq. (2.2). Note that when $p_1 = p_2 = 1/2$, E_r is constant and $D_q = 1$, and there is no intermittency.

In Burgers equation, the dissipation occurs only at the shocks, which are narrow regions. So, as we traverse along a line, there are regions of no dissipation, then suddenly a short region (shock) with intense dissipation appears. According to this observation, the noiseless Burgers equation exhibits strong intermittency, in fact maximal intermittency, in the light of Meneveau and Sreenivasan's model [29,30].

The structure function of the noiseless KPZ equation can be easily calculated using the relationship $h(x,t) = -\int^x u(x',t)\,\mathrm{d}x'$. The surface profile $h(x)$ at a asymptotic time

(shown in Fig. 1) is

$$h(x,t)=\begin{cases} -\frac{x^2}{2t}+\frac{\eta_i}{t}(x-\xi_i) & \text{for } \frac{1}{2}(\xi_{i-1}+\xi_i)<x<\xi_i\,, \\ -\frac{x^2}{2t}+\frac{\eta_{i+1}}{t}(x-\xi_i) & \text{for } \xi_i<x<\frac{1}{2}(\xi_i+\xi_{i+1})\,. \end{cases} \tag{2.6}$$

After some algebra we can obtain the structure function $T_q(r)$ for the KPZ equation:

$$T_q(r)\approx\frac{1}{(q+1)L}\left(\frac{r}{t}\right)^q\sum_i[(\eta_{i+1}-\xi_{i+1})^{q+1}-(\eta_{i+1}-\xi_i)^{q+1}]$$

$$+\frac{1}{(q+1)L}\left(\frac{r}{t}\right)^q r\sum_i\frac{[(\eta_{i+2}-2\xi_{i+1})^{q+1}-(\eta_{i+1}-2\xi_{i+1})^{q+1}]}{(\eta_{i+2}-\eta_{i+1})}\,. \tag{2.7}$$

The solution of the KPZ equation has cusps at positions where shocks appear in Burgers equation. These cusps yield contributions proportional to r^{q+1} to the structure function. Hence, to a leading order, $T_q(r)\propto r^q$. Therefore, $\zeta_q^{\mathrm{KPZ}}=q$. Note that smooth continuous curves also yield $\zeta_q=q$ because $h(x+r)-h(x)\approx h'r$ for small r. Since the exponent ζ_q^{KPZ} is proportional to q, the solution of the noiseless KPZ equation will be classified to be non-intermittent. However, note that the probability density of $h'=-u$ is flat (non-Gaussian), hence indicating intermittent behaviour for the noiseless KPZ equation. Clearly, there appears to be a contradiction because the structure function indicates non-intermittency, but the $P(h')$ indicates intermittency. The resolution of this apparent contradiction is given below.

The systems under investigation for intermittency have typically a random output. In non-intermittent systems, the probability density of the output is Gaussian, i.e., probability of finding a large signal decreases as $\exp(-x^2)$. However, in the intermittent systems, the probability density of the random output signal deviates from the Gaussian behaviour. The key is that the system under investigation for intermittency must have a random output, which is not the case for the noiseless KPZ and Burgers equation. In that sense, it is somewhat meaningless to ask whether the noiseless Burgers and KPZ equations exhibit intermittency or not. This is the reason why the conclusions from the structure function and those from the probability density differ for the noiseless KPZ equation. In literature, however, the noiseless Burgers equation is classified as an intermittent system.

In the following section we will derive the energy spectrum of the noiseless Burgers and KPZ equation using Eqs. (2.1) and (2.7).

3. Energy spectrum of noiseless Burgers and KPZ equation

We briefly discuss the energy spectrum of the noiseless Burgers and KPZ equation because they will be compared with the results obtained for the equations with coloured noise. We restate the earlier results by Kida [6], Gotoh [7], and Bouchaud et al. [8]. We can obtain the energy spectrum $E^u(k)=\langle|u(k)|^2/2\rangle$ using $S_2(r)$. Clearly,

$$\langle u(x+r)u(x)\rangle=\langle u^2\rangle-\tfrac{1}{2}S_2(r)\,. \tag{3.1}$$

Therefore,

$$E(k) = \frac{1}{L}\int_{-\infty}^{\infty} 1/2\langle u(x+r)u(x)\rangle \exp(-ikr)\,\mathrm{d}r$$

$$= \delta_{k,0}\frac{\langle u^2\rangle}{2} + \frac{1}{2Lt^2}\frac{\mathrm{d}^2\delta_{k,0}}{\mathrm{d}k^2} + (Lk)^{-2}\sum_i \mu_i^2\,. \tag{3.2}$$

Hence, the noiseless Burgers equation has energy spectrum $E^u(k) \propto k^{-2}$ for $k > 0$. In the above equation, the Fourier transform of r^2 is $\mathrm{d}^2\delta_{k,0}/\mathrm{d}k^2$ [31].

A similar procedure using $T_2(r)$ will yield $E^h(k) = \langle |h(k)|^2/2\rangle$,

$$E^h(k) = \delta_{k,0}\frac{\langle h^2\rangle}{2} + B\frac{\mathrm{d}^2}{\mathrm{d}k^2}\delta_{k,0} + \frac{C}{(Lt)^2}k^{-4}\,, \tag{3.3}$$

where B and C are constants [31]. Hence for $k > 0$, we obtain $E^h(k) \propto k^{-4}$ for the noiseless KPZ equation.

Most papers in the past implicitly assume that if $T_2(r) \propto r^{2\chi}$, then $E^h(k)$ should be proportional to $k^{-2\chi-1}$. Clearly this does not hold for the noiseless KPZ equation (check: $\chi = 1$, but $E^h(k) \propto k^{-4}$). These apparent contradictions, which also occur for $\sigma > 1$, can be resolved using the following arguments.

Suppose $E(k) = Ak^{-2\chi-1}$. The second-order structure function $S_2(r)$ is given by

$$S_2(r) = \frac{1}{L}\int_0^L \mathrm{d}x\langle |u(x+r) - u(x)|^2\rangle$$

$$= 16\int_0^\infty \mathrm{d}k\, E(k)\sin^2(kr/2)$$

$$= 16\int_0^\infty \mathrm{d}k\, Ak^{-2\chi-1}\sin^2(kr/2)\,. \tag{3.4}$$

We are interested in the leading-order behaviour of $S_2(r)$ for small r. When $\chi < 1$, the above integral converges, and

$$S_2(r) \propto 16Ar^{2\chi}\int_0^\infty \mathrm{d}s\, s^{-2\chi-1}\sin^2(s)$$

$$\approx AC_1 r^{2\chi}\,, \tag{3.5}$$

where C_1 is a dimensionless constant. When $\chi > 1$, the integral diverges from below (small k). However, we can cure this divergence by choosing the lower limit of the integral to be $2\pi/L$, which yields

$$S_2(r) \propto 16A\int_{2\pi/L}^\infty \mathrm{d}k\, k^{-2\chi-1}(kr/2)^2$$

$$\approx AC_2(r/L)^2 L^{2\chi}\,, \tag{3.6}$$

where C_2 is a constant.

Hence, when $\chi < 1$, $E(k) \propto k^{-2\chi-1}$ and $S_2(r) \propto r^{2\chi}$ as expected, however when $\chi > 1$, $E(k) \propto k^{-2\chi-1}$ and $S_2(r) \propto r^2$. This analytical results are seen in our numerical simulations to be described below.

After the discussion on the noiseless equation, now we turn to the noisy Burgers and KPZ equations.

4. Noisy Burgers equation: various ranges of parameters σ

In this section we will attempt to divide the parameter range of σ according to the properties of the solution. From Eq. (1.1) the noise spectrum $|\zeta(k)|^2$ is proportional to $k^{-2\sigma}$. Using this we can derive the noise–noise correlation as

$$\langle\zeta(x,t)\zeta(x+r,t)\rangle \sim \begin{cases} B_0\delta(r) & \text{for } \sigma = 0\,, \\ B_1 - C_1 r^{2\sigma-1} & \text{for } 0 \leqslant \sigma \leqslant 1/2\,, \\ B_2 - C_2 \log(r) & \text{for } \sigma = 1/2\,, \\ B_3 - C_3 r^{2\sigma-1} & \text{for } 1/2 < \sigma \leqslant 3/2\,, \\ B_4 - C_4 r^2 L^{2\sigma-3} & \text{for } \sigma > 3/2\,, \end{cases} \tag{4.1}$$

where L is the length of the system, and B_i and C_i are constants. For $-1 \leqslant \sigma \leqslant 0$, $|\zeta(k)|^2 \to \infty$ for large k, hence, the inverse Fourier transform which yields $\langle\zeta(x,t)\zeta(x',t)\rangle$ is not defined in this regime. However, Kardar et al. [9] and Medina et al. [10] have solved the KPZ equation for this regime using $|f(k)|^2$ which is well defined for large k. We call the region $-1 \leqslant \sigma \leqslant 0$ as (a).

It can be deduced from the above discussion that the noise–noise correlation increases with the increase of σ till $\sigma = 3/2$. Beyond $\sigma = 3/2$, the correlation is proportional to $1 - Cr^2$ for all σ. Therefore, it is expected that the $h - h$ and $u - u$ correlation would increase with the increase of σ till 3/2, beyond which the behaviour is expected to be somewhat similar. Keeping this in mind we have divided the σ range beyond 0 in two regions: (b) $0 \leqslant \sigma \leqslant 3/2$, and (c) $\sigma > 3/2$. Well-defined shocks develop in the parameter range (c) due to the large noise–noise correlation, and these shocks determine the exponents. In the intermediate parameter range (b), the exponents change slowly from RG-dominated values to shock dominated values. The details are given in the next section.

Polyakov [2] has analytically solved Burgers equation with $\sigma = 3/2$ using the methods of quantum field theory. Boldyrev [14,15] extended Polyakov's method to the range $1/2 \leqslant \sigma \leqslant 3/2$ and derived the spectral exponents and the probability densities. Boldyrev derived that $\chi = 1 + 2\sigma/3$ for $1/2 \leqslant \sigma \leqslant 3/4$, and $\chi = 3/2$ for $\sigma > 3/4$. Boldyrev [14] suggests that the above formula may also be valid for $0 \leqslant \sigma \leqslant 1/2$. In the following section we will compare our numerical results with the theoretical predictions of Medina et al. [10], Polyakov [2], and Boldyrev [14,15].

5. Simulation method

Our calculations in this paper have been done using direct numerical simulations based on pseudo-spectral method. This method, commonly used in turbulence

simulations, is expected to perform better than finite-difference scheme because the derivatives can be calculated exactly in the spectral method [32]. The finite-difference scheme was adopted by Moser et al. [33] and Peng et al. [24] in their simulation of KPZ equation for $-1 \leqslant \sigma \leqslant 0$.

We solve the KPZ equation in one dimension. The details of the simulation are as follows. A box of size 2π is discretized into $N = 1024$ divisions. The KPZ equation is solved in Fourier space. However, to compute the nonlinear term, we go to real space, perform multiplication, then again come back to Fourier space. We time advance the Fourier components $h(k,t)$ using Adam Bashforth time-marching procedure with flat surface as an initial condition. Two-third rule is used to remove aliasing [32]. For details of the simulation refer to Canuto et al. [32] and Verma et al. [34]. In our simulation we also add hyperviscosity term ($\kappa\nabla^4 h$) to the KPZ equation to damp the large wavenumber modes strongly. The hyperviscosity term does not affect the intermediate scales which is of our interest [34]; this is because the $\nabla^4 h$ and higher order derivative terms are irrelevant in the renormalization group sense (cf. Barabasi and Stanley [12] and references therein).

In our simulation we take v and κ to be very small. Note that large v corresponds to Edward–Wilkinson (EW) equation. The dimensionless parameters used in our simulations are

$$\lambda = 1.0\,,$$

$$v = 10^{-5}\,,$$

$$\kappa = 10^{-6}\,,$$

$$(2\pi)^2 D = 10^{-3}\,,$$

$$\mathrm{d}t = 1/2000 \tag{5.1}$$

with one exception. For $\sigma = -1$, we choose $\lambda = 0.1$ for the stability of the code. In Appendix A we have varied values of the parameters v and D and shown crossover from KPZ behaviour to EW equation.

The values of σ used in our simulation are $-1, -0.85, -0.75, -0.60, -0.50, -0.25, 0$, $1.25, 1.50, 1.75, 1, 2$, and 6. We have time evolved the equation till 15 nondimensional time units. We find that the system reaches saturation in approximately 8 to 10 time units. For reference, 2π time unit corresponds to one eddy turnover time in fluid turbulence. For ensemble averaging, we have performed averages over 100 samples which start with different random seeds for the noise. We have used *ran*1 of numerical recipes [35] as our random number generator. Each computer run for 15 time units and 100 samples takes approximately 7 h on a Pentium machine (150 MHz).

We have calculated χ and β using the simulation data. The ensemble average $\langle . \rangle$ have been obtained by taking averages over 100 runs. The width $W(L,t) = [\langle \sum_x h^2(x)/N \rangle]^{1/2}$ grows as a power law in time, i.e., $W(L.t) \propto t^{\beta_{\mathrm{KPZ}}}$, in the early stages of growth. We obtain β_{KPZ} by fitting a straight line in log–log plot of $W(L,t)$ vs. t over a range

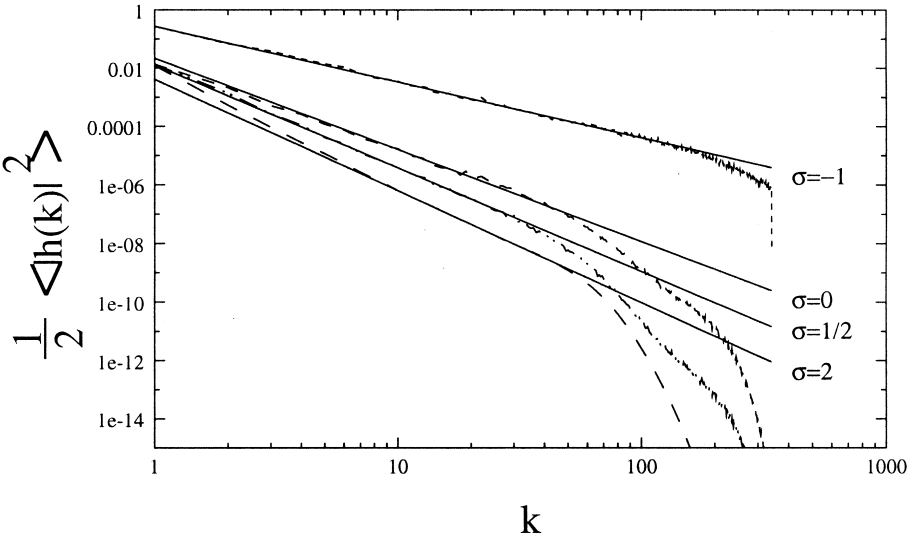

Fig. 3. The energy spectrum $(1/2)\langle|h(k)|^2\rangle$ vs. k for the KPZ equation when $\sigma=-1,0,1/2,2$. The lines of best fit for the intermediate range of k are also shown.

of $t=0.2:2.5$. The other exponent χ_{KPZ} is obtained from the asymptotic $\langle|h(k,t)|^2\rangle$ averaged over 100 runs. We find that power law holds ($|h(k)|^2 \propto k^{-2\chi_{\mathrm{KPZ}}-1}$) for $k=10:8$; this range corresponds to the inertial range of turbulence. We perform the averaging at steady state ($t=15$). In Fig. 3 we plot $\langle|h(k)|^2\rangle$ vs. k for $\sigma=-1,0,1/2$, and 2. The lines of best fit are also shown in the figure. The computed values of the exponents are listed in Table 1. Our estimate of the error in the exponent is roughly 0.05.

We have also calculated the structure functions $S_q(r)$ and $T_q(r)$ using the simulation data. The variable r ranges from 1 to $N/2$. Near the boundaries we calculate Δu or Δh using wrap around scheme, i.e., $x+r$ is taken as $\mathrm{mod}(x+r,N)$. We have reported the structure function exponents at the steady state ($t=15$).

The probability densities $P(h), P(u)$, and $P(u')$ have been calculated by averaging the histograms over 100 runs at every 0.2 time interval from initial time of 5 units to the final time of 15 units. Even though the solution has not reached the steady state at $t=5$, for more sampling we have taken the time interval from $t=5$ to 15.

In the following section we will describe the results of our simulation for various degrees of noise correlations, i.e., for different σ.

6. Simulation results

As discussed in Section 4, we divide the range of parameter σ into three regions: (a) $-1\leqslant\sigma\leqslant 0$, (b) $0\leqslant\sigma\leqslant 3/2$, and (c) $\sigma\geqslant 3/2$. Fig. 4 shows numerical $u(x,t)$ for

Table 1
The exponents α and β for KPZ equation for various σ's. The Medina et al. exponents are also listed for comparison

$\sigma = \rho - 1$	Our results		Medina et al.'s results	
	α_{KPZ}	β_{KPZ}	α_{KPZ}	β_{KPZ}
−1.00	0.46	0.35	0.50	0.33
−0.85	0.50	0.28	0.50	0.33
−0.75	0.53	0.31	0.50	0.33
−0.60	0.60	0.33	0.60	0.43
−0.50	0.70	0.36	0.67	0.50
−0.25	0.89	0.42	0.83	0.71
0.00	1.07	0.45	1.00	1.00
0.25	1.15	0.50	—	—
0.50	1.27	0.48	—	—
0.75	1.31	0.50	—	—
1.00	1.58	0.48	—	—
2.00	1.54	0.48	—	—
6.00	1.45	0.48	—	—

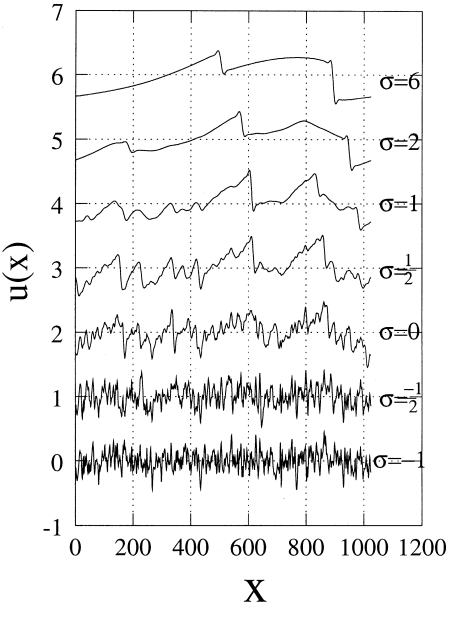

Fig. 4. The normalized velocity profile $u(x)$ vs. x for Burgers equation when $\sigma = -1, -1/2, 0, 1/2, 1, 2, 6$. The profile is noisy for $-1 \leqslant \sigma \leqslant 0$, has only well-developed shocks for $\sigma \geqslant 3/2$, and has both fluctuations and shocks for the intermediate range of σ.

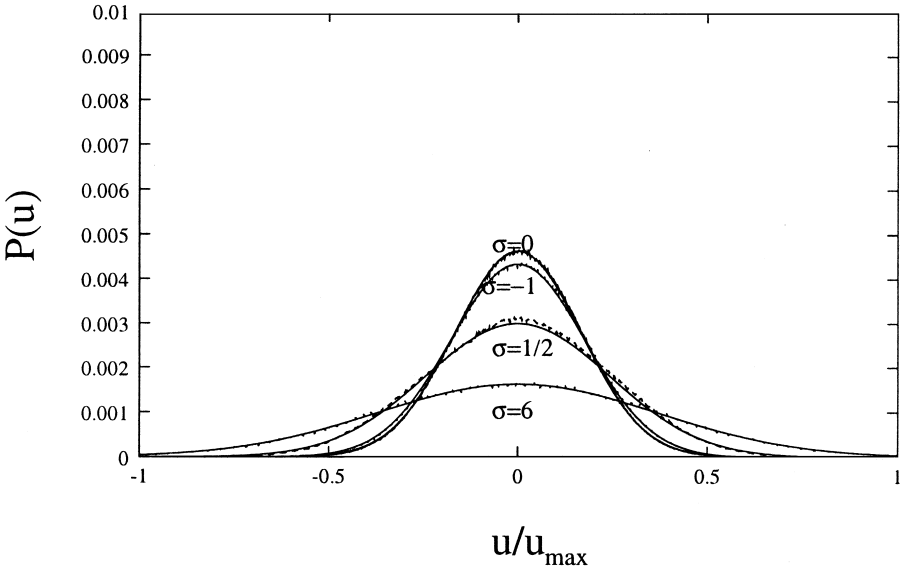

Fig. 5. The probability density $P(u)$ vs. $u/u_{\max}$ for $\sigma = -1, 0, 1/2$ and 6. The best fit Gaussian curves are also shown in the figure.

various σ's. We find that noise dominates when σ is negative. However, shock-like structures are clearly visible for $\sigma = 2, 6$ (compare with Fig. 1). In the the intermediate range of σ (region (b)), both noise and shock structure coexist. We show below that the structures present in the profile contribute significantly to the determination of the spectral and intermittency exponents.

Regarding energy spectrum, our numerical results are in good agreement with the RG predictions for $-1 \leqslant \sigma \leqslant 0$ or $0 \leqslant \rho \leqslant 1$. There is a gradual transition from $\chi_{\mathrm{KPZ}} = 1$ to $\chi_{\mathrm{KPZ}} = 3/2$ as σ increases from 0 to 3/2. For $\sigma \geqslant 3/2$ we find that $\chi_{\mathrm{KPZ}} = 3/2$.

Regarding probability density, we find that the probability densities $P(h)$ and $P(u)$ are Gaussian for all σ's. Fig. 5 shows the plot of $P(u)$ vs. u along with the best fit Gaussian curves. Clearly $P(u)$ is Gaussian for all the σ's. Therefore, the exponents of the structure functions $T_q(r)$ are expected to be proportional to q.

Fig. 6 shows a typical log–log plots of $S_q(r)$ and $T_q(r)$ vs. r (here shown for $\sigma = 6$). The shock region is $r < 10$ where both $S_q(r)$ and $T_q(r)$ are proportional to r^q because $u(x)$ and $h(x)$ are continuous here. The region of our interest is $r = 10 : 80$ where both $S_q(r)$ and $T_q(r)$ are power laws. The exponents for this range of r, ζ_q^{Burg} and ζ_q^{KPZ}, are listed in Tables 2 and 3, respectively. Fig. 7 shows ζ_q^{KPZ} vs. q plot, and Fig. 8 shows ζ_q^{Burg} vs. q plots. Clearly, ζ_q^{KPZ} is approximately proportional to q as predicted in the previous paragraph. Hence, our results regarding $P(u)$ and $T_q(r)$ are consistent.

We find, however, that $P(u')$ deviates significantly from the Gaussian behaviour as we increase σ from 0, thus signalling an intermittent behaviour for u. The details of our results for various ranges are given below.

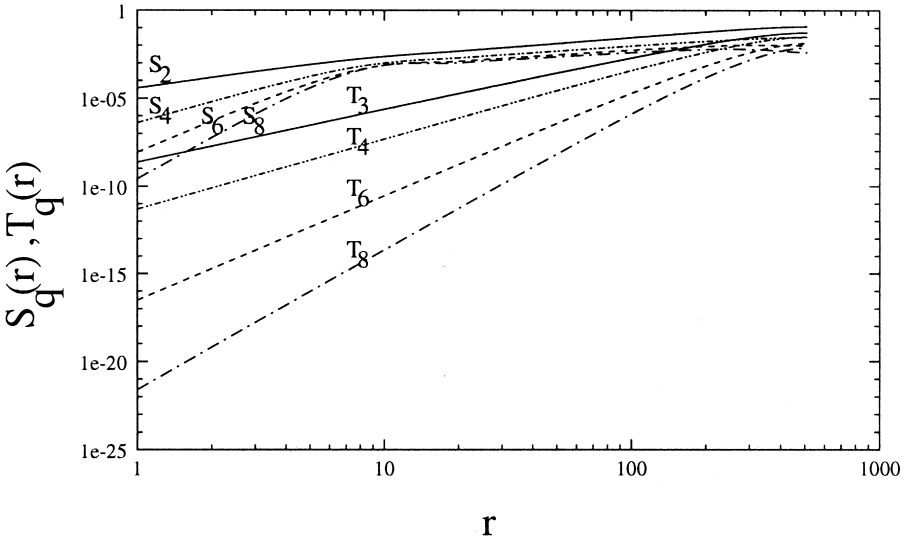

Fig. 6. The structure functions $S_q(r), T_q(r)$ vs. r for $\sigma = 6$.

Table 2
The structure function exponents ζ_q^{Burg} of $\langle |u(x+r) - u(x)|^q \rangle$ for the Burgers equation for various σ's

$q \setminus \sigma = \rho - 1$	-1	$-3/4$	$-1/2$	$-1/4$	0	1/4	1/2	2	6
1	−0.012	−0.001	0.017	0.069	0.16	0.29	0.42	0.90	0.94
2	−0.020	0.001	0.041	0.136	0.30	0.51	0.70	1.09	1.09
3	−0.024	0.006	0.068	0.197	0.41	0.63	0.84	1.00	1.00
4	−0.024	0.014	0.099	0.250	0.50	0.65	0.85	0.94	0.96
5	−0.020	0.024	0.130	0.293	0.55	0.58	0.81	0.90	0.93
6	−0.013	0.036	0.161	0.329	0.58	0.47	0.74	0.85	0.89
7	0.003	0.052	0.191	0.358	0.60	0.34	0.66	0.81	0.84
8	0.009	0.071	0.218	0.383	0.62	0.20	0.57	0.78	0.79

6.1. $-1 \leqslant \sigma \leqslant 0$

In Table 1 we have listed our numerical values of χ_{KPZ} and β_{KPZ}. For comparison we also list the predicted values of Medina et al. [10] below:

$$\chi = \begin{cases} \frac{1}{2} & \text{for } -1 \leqslant \sigma \leqslant -\frac{3}{4}, \\ 1 + \frac{2}{3}\sigma & \text{for } -\frac{3}{4} \leqslant \sigma \leqslant 0 \end{cases} \tag{6.1}$$

and

$$\beta = \begin{cases} \frac{1}{3} & \text{for } -1 \leqslant \sigma \leqslant -\frac{3}{4}, \\ \frac{3+2\sigma}{3-2\sigma} & \text{for } -\frac{3}{4} \leqslant \sigma \leqslant 0. \end{cases} \tag{6.2}$$

The Medina et al. results are based on RG scheme that breaks down beyond $\sigma = 0$.

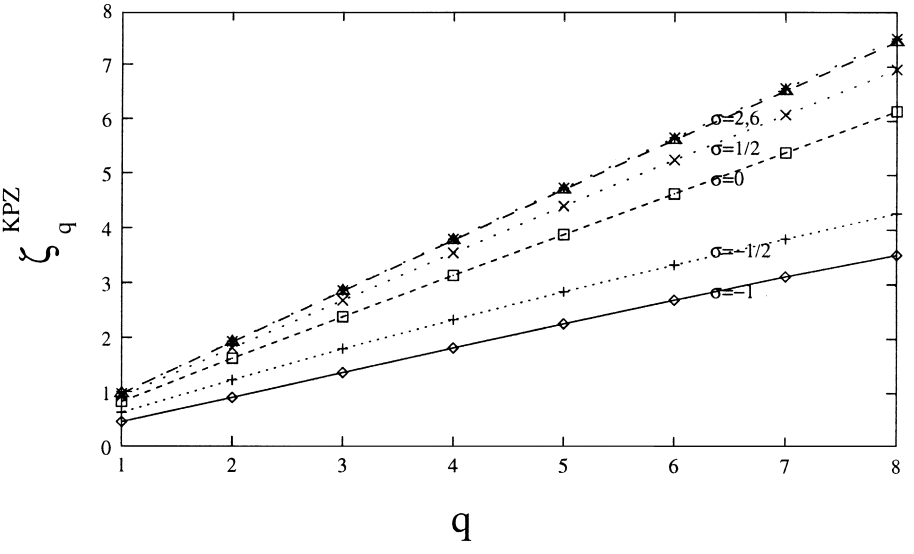

Fig. 7. The exponent ζ_q^{KPZ} vs. q for $\sigma = -1, -1/2, 0, 1/2, 2, 6$.

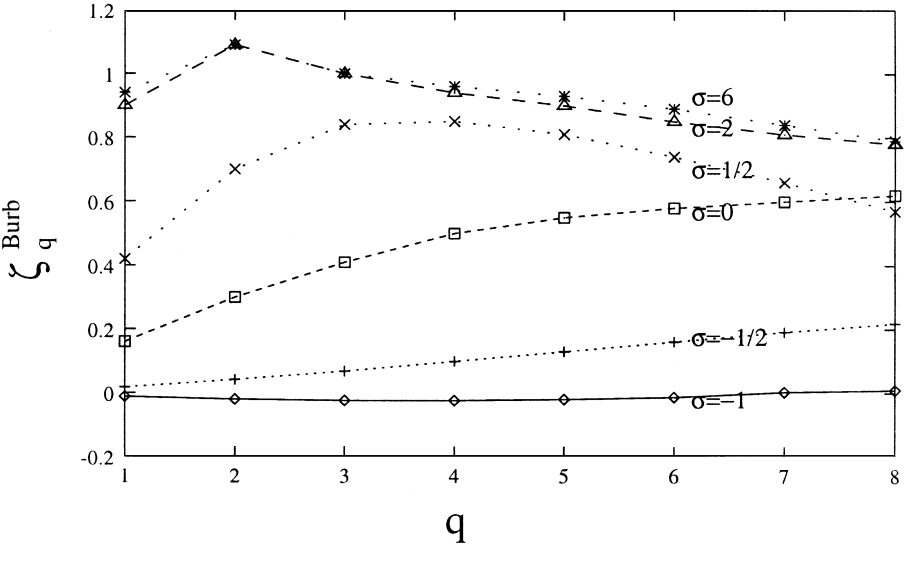

Fig. 8. The exponent ζ_q^{Burg} vs. q for $\sigma = -1, -1/2, 0, 1/2, 2, 6$.

We compute χ_{KPZ} by a straight line fit to the log–log plot of $\langle |h(k)|^2 \rangle$ over $k = 10 : 80$ at $t = 15$ (see Fig. 3). Note that $|h(k)|^2 \propto k^{-2\chi-1}$. The χ_{KPZ}s listed in Table 1 show that that our numerical χ_{KPZ}s are in close agreement with the Medina et al. [10] and the Chattopadhyay and Bhattacharjee [11] theoretical predictions. Our findings are also consistent with earlier simulation results by Amar et al. [25], Peng et al. [24], and

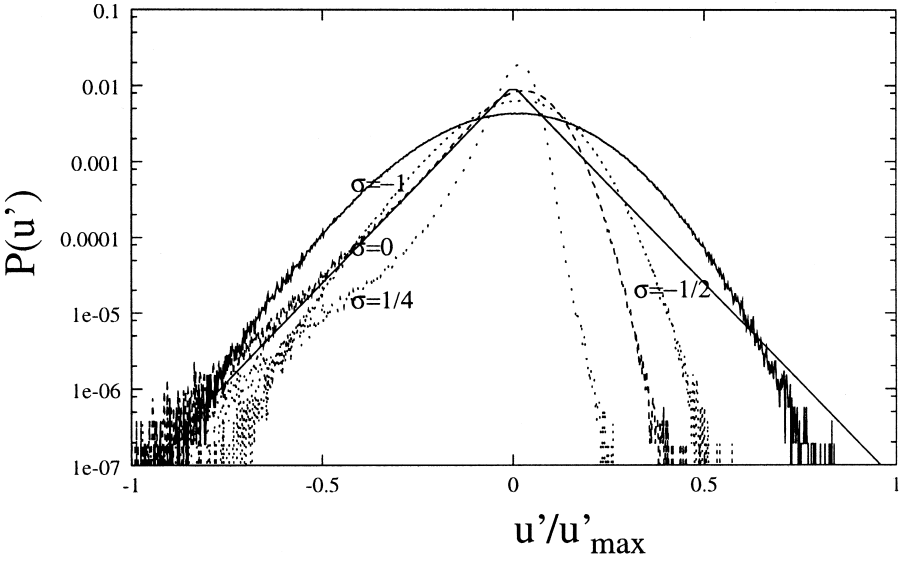

Fig. 9. The probability density $P(u')$ vs. $u'/u'_{\max}$ for $\sigma=-1,-1/2,0$ and $1/4$. Function $0.01\exp(-0.14|u'|)$ fits well for $\sigma=0$.

Meakin and Jullien [26,27]. For $\sigma=-1/4$, Hayot and Jayaprakash [3] have reported a crossover in the wave number space — from RG dominated region for small k to free field behaviour for large k. We do not find any such crossover in our simulation. Regarding the Burgers equations, $\chi_{\rm Burg}=\chi_{\rm KPZ}-1$.

Regarding $\beta_{\rm KPZ}$ calculations, our results are in agreement with the Medina et al. predictions for $\sigma=-1:-3/4$. However, our exponents differ significantly with the Medina et al. exponents for higher σ's. For example, for $\sigma=0$, we obtain $\beta_{\rm KPZ}=0.45$ contrary to the predicted $\beta_{\rm KPZ}=1$. The reason for this discrepancy is not clear to us at this point. Regarding $\beta_{\rm Burg}$, we find that it is approximately 0.5, consistent with the Hayot and Jayaprakash findings [3].

The probability density $P(u')$ vs. u' for $\sigma=-1,-1/2,0$ is shown in Fig. 9 on a semilog plot. The figure shows that $P(u')$ is Gaussian for $\sigma=-1$, but it deviates from the Gaussian behaviour with the increase of σ; the deviations becomes more and more prominent for higher σ. At $\sigma=0$, $P(u')\approx 0.01*\exp(-0.14|u'|)$ for negative u' (the curve of the best fit shown in the Fig. 9). Beyond $\sigma=0$, a powerlaw tails start appearing for negative u'.

Table 2 and Fig. 8 show that $\zeta_2^{\rm Burg}$ is close to zero for $\sigma<0$. The energy spectrum $\langle|u(k)|^2/2\rangle \propto k^{-2\chi_{\rm KPZ}+1}$. Therefore, using the arguments of Section 3 we can easily show that $\langle|u(x+r)-u(x)|^2\rangle \propto r^{2(\chi_{\rm KPZ}-1)}$ for $\sigma<0$. For $\sigma=0$, it can be easily shown that $\langle|u(x+r)-u(x)|^2\rangle \propto \log(r)$. We find in our simulation that $\zeta_2^{\rm KPZ}$ is positive contrary to the above prediction. This deviation may be because of *intermittency* (due to the presence of small shocks). It is also possible that at large r ($r\approx L$), the other sub-critical terms may become comparable to the leading-order term and may change

the exponent. Quantitative calculation of the exponents for this range of σ is beyond the scope of this paper.

6.2. $\sigma \geqslant 3/2$

One of the important aspect of this paper is the discussion of the energy spectrum, probability density and structure functions of the Burgers equation with large σ. As shown in Fig. 4, shocks are prominent for this range of σ. Due to these shocks, the exponent $\chi_{\mathrm{KPZ}} \approx 3/2$ for $\sigma > 3/2$ (see Table 1 and Fig. 3). Note that $\chi_{\mathrm{KPZ}} = 3/2$ and $\chi_{\mathrm{Burg}} = 1/2$ for the noiseless Burgers equation due to the presence of shocks.

The existence of shocks for large σ can be argued from the noise–noise correlation discussed in Section 4. For large σ, there is long-ranged noise–noise correlation. Physically, large fluid parcels are moved around by this noise. As a consequence, there will be regions where the parcels forced by oppositely directed noise collide with each other and create "strong" shocks. Hence, it is not surprising that strong shocks will be generated for large σ. These shocks determine the dynamics and the spectral indices of Burgers and KPZ equations. Therefore, the noisy KPZ equation with large σ yields the same energy spectrum and multiscaling exponents as the noiseless KPZ equation.

The noise–noise correlation is proportional to $1 - Cr^2$ for all $\sigma \geqslant 3/2$, hence the spectral and multiscaling exponents are expected to be somewhat similar for all the σ beyond $3/2$. This is borne out by our numerical simulation. This is consistent with the trivial observation that for large σ only $k = 1$ mode is effective. It is interesting to note that $k = 1$ mode (i.e., $\zeta(x) = \sin(x)$) also yields noise–noise correlation proportional to $1 - Cr^2$, and approximately the same exponents as those with $\sigma \geqslant 3/2$.

We have also analysed the stability of the shocks at a preliminary level. For large σ, the significant contribution to the dynamics comes only from the $k = 1$ mode of the noise. Since the first mode ($k = 1$) is noisy, the formation of a single shock delayed for some time because of the movement of the zero of the noise signal. However, after the shock is formed, it shifts around by only a small amount because the impulse due to the random noise is not strong enough to move the shock by a large distance.

We have also calculated β for both Burgers and KPZ equations when $\sigma > 3/2$ and found them to be approximately 1/2 . This result is consistent with findings of Hayot and Jayaprakash [3].

Regarding the intermittency exponents, as shown in Fig. 8, $\zeta_q^{\mathrm{Burg}} \approx 1$ for all q for $\sigma \geqslant 3/2$. This result is consistent with existence of shocks (see Fig. 4 and Section 2). For large r, $S_q(r)$ is not proportional to r. This is because of the term similar to $(\mu_i - r/t)^q$ of Eq. (2.1), which becomes important at large r. The effects of this subcritical term is evident in the intermittency exponents listed in Table 2. We had anticipated ζ_q^{Burg} to be 1, but we consistently find them to be less than 1. The same trends were observed for the noiseless case.

Fig. 10 shows the probability density $P(u')$ for various σ's. The curves of best fit are also shown in the figure. The probability density is clearly non-Gaussian for all σ's shown in the figure. In our simulations we find that for all $\sigma \geqslant 3/2$,

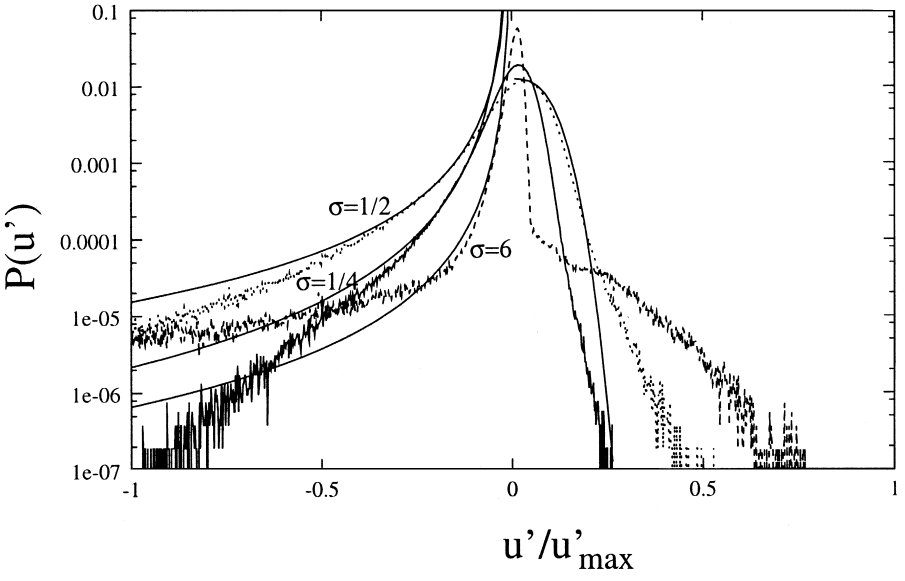

Fig. 10. The probability density $P(u')$ vs. $u'/u'_{\max}$ for $\sigma = 1/4, 1/2, 6$. The best fit curves for negative u' are: $u'^{-2.85}$ for $\sigma = 1/4$, $u'^{-2.2}$ for $\sigma = 1/2$, and $u'^{-2.5}$ for $\sigma = 6$. For positive u', $\exp(-Cx^3)$ fits well for $\sigma = 1/2$.

$P(u') \propto u'^{-\alpha}$ ($\alpha = 2.2 - 2.5$) fits quite well with the numerical $P(u')$ for the intermediate range of the negative u'. This result is in agreement with the Polyakov's theoretical prediction for $\sigma \geqslant 3/2$ [2]. Curiously, $P(u')$ for $u' > 0$ is also non-Gaussian, but it does not match with the Polyakov's predictions for positive u'.

We have shown in this section that both noiseless Burgers equation and the Burgers equation with strongly correlated noise have $S_q(r) \propto r$. However, the probability densities $P(u)$ and $P(u')$ are very different for these two cases (see Figs. 2 and 10). This difference is because of the different nature of the noise.

The entries in Table 2 show that $\zeta_q^{\mathrm{KPZ}} = q$. This can be argued as follows. Since $\chi_{\mathrm{KPZ}} \approx 3/2$, the second-order structure function $T_2(r)$ will be proportional to r^2, or $\zeta_2^{\mathrm{KPZ}} = 2$ (see Section 3). This is seen in our simulation for $\sigma \geqslant 3/2$. Fig. 5 also shows that $P(u)$ is Gaussian. Therefore, $T_q(r) \propto [T_2(r)]^{q/2} \propto r^q$, hence $\zeta_q^{\mathrm{KPZ}} = q$, a result seen in our numerics. Thus, structure function and energy spectrum calculations are consistent.

After discussing the shock-dominated region of $\sigma \geqslant 3/2$, we turn to the region $0 \leqslant \sigma \leqslant 3/2$.

6.3. $0 < \sigma \leqslant 3/2$

The χ_{KPZ} calculated by our numerical simulation for the range $0 \leqslant \sigma \leqslant 3/2$ is listed in Table 1. The exponent increases from 1 and saturate at 3/2. That is, there is a gradual shift from RG-dominated exponents to shock-dominated exponents as we vary σ. The

Table 3
The structure function exponents ζ_q^{KPZ} of $\langle|h(x+r)-h(x)|^q\rangle$ for the KPZ equation for various σ's

$q \setminus \sigma = \rho - 1$	-1	$-3/4$	$-1/2$	$-1/4$	0	1/4	1/2	2	6
1	0.45	0.50	0.62	0.73	0.82	0.88	0.92	0.97	0.97
2	0.90	1.00	1.22	1.44	1.62	1.73	1.81	1.92	1.93
3	1.36	1.49	1.80	2.12	2.39	2.55	2.69	2.86	2.87
4	1.82	1.97	2.34	2.78	3.15	3.36	3.56	3.79	3.81
5	2.27	2.44	2.86	3.42	3.90	4.17	4.42	4.72	4.75
6	2.71	2.90	3.35	4.04	4.65	4.98	5.27	5.64	5.68
7	3.14	3.38	3.83	4.65	5.41	5.78	6.11	6.55	6.60
8	3.54	3.85	4.30	5.28	6.18	6.58	6.95	7.46	7.52

profile $u(x,t)$ of Fig. 4 shows that both fluctuations and shocks coexist in this range, with shocks becoming more and more important as σ increases.

Boldyrev [14,15] has calculated χ_{KPZ} using methods of quantum field theory and derived that $\chi_{\mathrm{KPZ}} = 1 + 2\sigma/3$ for $1/2 \leqslant \sigma \leqslant 3/4$, and $\chi_{\mathrm{KPZ}} = 3/2$ for $\sigma > 3/4$. Boldyrev [14] suggests that the above formula may be valid for $0 \leqslant \sigma \leqslant 3/2$. Comparison of Boldyrev's predictions with the entries of Table 1 shows that the predictions work quite well till $0 \leqslant \sigma \leqslant 1/2$. After that there is a significant deviation, and the exponents appear to be outside the numerical error bars. We need to probe the region $1/2 \leqslant \sigma \leqslant 3/4$ carefully to reach a definite conclusion.

We presume that both fluctuations and the embedded structures are important in the determination of the spectral index. One would need to combine contributions from the structures and fluctuations to obtain the energy spectrum [36]. In Appendix B we sketch an elementary framework when both structure and fluctuations are present in the system.

The Burgers equation for $\sigma = 1/2$ has been studied extensively by Chekhlov and Yakhot [1]. They find in their high-resolution simulation that $|u(k)|^2 \propto k^{-5/3}$. The spectrum in our low-resolution simulation is $|u(k)|^2 \propto k^{-1.54}$ ($\chi_{\mathrm{KPZ}} = 1.27$), which is close to the Chekhlov and Yakhot [1] result. Chekhlov and Yakhot [1] have argued for a constant cascade of energy in the wavenumber space in this case and claimed that the Kolmogorov-like energy spectra is due to the constancy of the energy flux. However, we find the cascade rate to be constant for all $\sigma > 1/2$, but the spectral index of the energy spectrum is in the range of 5/3 to 2 (to be discussed in Section 7). Hence, the argument that the constant flux yields Kolmogorov's spectrum is incorrect.

Regarding the probability distribution, in Fig. 10 we plot $P(u')$ vs. u' along with the curves of best fit. It is found that $P(u')$ is a power law for $u' < 0$. For $\sigma = 1.25$, $P(u') \propto u'^{-2.86}$, but for $\sigma = 1/2$, $P(u') \approx u'^{-2.2}$, with an error of approximately 10% for both the cases. Curiously, Polyakov's predictions ($\sigma = 3/2$) for positive u' appears to be applicable only for $\sigma = 1/2$; here $P(u') \propto \exp(-Cx^3)$.

The roughening exponents χ_{KPZ} lie between 1 and 3/2. Therefore, ζ_q^{KPZ} should be proportional to q as argued in the previous subsection. Our numerical simulations yield approximately the same exponents (see Table 3). Hence, our energy spectrum calculations and the structure function calculations are consistent.

6.4. Summary of simulation results

From the above discussion we see that Burgers and KPZ equations are well understood for $-1 \leqslant \sigma \leqslant 0$ and $\sigma > 3/2$. In the intermediate range $0 < \sigma < 3/2$, Boldyrev's predictions appear to explain the numerical data in part of the regime; further analytic and numerical work is required in this regime.

For all $\sigma > -1/2$, $\chi_{\mathrm{KPZ}} + z$ ($z = \chi_{\mathrm{KPZ}}/\beta_{\mathrm{KPZ}}$) deviates significantly from 2. In fact, for larger σ, $\chi_{\mathrm{KPZ}} + z = 3/2 + (3/2)/(1/2) = 9/2$, quite far from 2. Note that Medina et al. [10] argue that the identity $\chi_{\mathrm{KPZ}} + z = 2$ is a consequence of Galilean invariance. However, Hayot and Jayprakash [3], Polyakov [2] and others have speculated violation of this identity due to the presence and motion of the shocks. The Meakin and Jullien [26,27] results also violate $\chi_{\mathrm{KPZ}} + z = 2$ condition for a range of σ. They find that for $\sigma = -1/4$, $\chi_{\mathrm{KPZ}} + z = 2.37$, quite different from 2. The violation of Galilean invariance even in the region $-1 \leqslant \sigma \leqslant 0$ signals importance of structures [2].

We also show that $P(u)$ is Gaussian for all σ. However, $P(u')$ is Gaussian at $\sigma = -1$, but continuously changes to $\exp(-x)$ then to a power law behaviour. Therefore, u field of Burgers equation exhibits intermittency. The degree of intermittency depends on σ.

The energy flux play an important role in turbulence analysis. In the following section we briefly report energy flux studies for the Burgers equation.

7. Energy flux of noisy Burgers equation

We derive an equation which gives us the energy transfer from the region $|k| \leqslant K$. The derivation of the energy equation from Eq. (1.1) and averaging yields [37]

$$\frac{\partial}{\partial t}\int_0^K E(k)\,\mathrm{d}k = -\int_0^K 2\nu k^2 E(k)\,\mathrm{d}k - \int_0^K \Re\left\langle u^*(k)\left[FT\left(\frac{\partial}{\partial x}u^2/2\right)\right]_k\right\rangle + \int_0^K \Re\left\langle u^*(k) f(k)\right\rangle . \tag{7.1}$$

From this equation, clearly the energy dissipation in the wavenumber sphere of radius K is

$$D_K = \int_0^K 2\nu k^2 E(k)\,\mathrm{d}k\,, \tag{7.2}$$

and the energy flux coming out of the wavenumber sphere of radius K is

$$\Pi_k = \int_0^K \Re\left\langle u^*(k)\left[FT\left(\frac{\partial}{\partial x}u^2\Big/2\right)\right]_k\right\rangle . \tag{7.3}$$

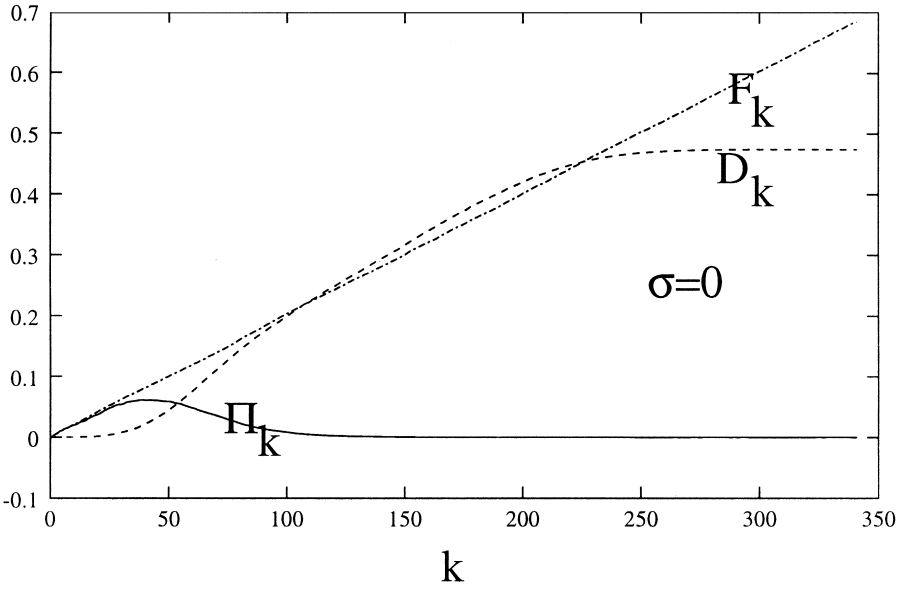

Fig. 11. The dissipation rate D_K, the energy flux Π_K, and the forcing rates F_K vs. K for $\sigma = 0$.

It can be easily seen that for the random noise, the energy supplied by the forcing to the wavenumber sphere of radius K is [37]

$$F_K = \int_0^K \Re \langle u^*(k) f(k) \rangle$$
$$= \int_0^K \langle |f(k)|^2 \rangle \, . \tag{7.4}$$

From Eq. (7.1) it is clear that at the steady state

$$F_K = \Pi_K + D_K \, . \tag{7.5}$$

We have plotted D_K, Π_K, and F_K for various σ. Fig. 11 shows the plots for $\sigma = 0$. Here, we find that $D_K \approx F_K$ till $k \approx 250$, but $\Pi_K \ll F_K$ except for small k. Similar results are obtained for all $-1 \leqslant \sigma \leqslant 0$.

Fig. 12 shows the plots of D_K, Π_K, and F_K for $\sigma = 1/2$. The forcing rate F_K is proportional to $\log K$. We also find a range of K for which Π_K is constant. These results are consistent with the findings of Chekhlov and Yakhot [1]. Fig. 13 shows the plot of the above quantities for $\sigma = 6$. Here again Π_K is constant for a range of K. An interesting point to note is that for $\sigma = 6$, F_K is constant beyond $K = 10$ or so; this is because effectively only first few modes are forced when σ is large. Similar results are obtained for all $\sigma \geqslant 2$.

We find that the energy flux is constant for the noisy Burgers equation for all $\sigma \geqslant 1/2$. However, the energy spectrum varies from $k^{-5/3}$ to k^{-2} as we increase σ from 1/2 to 3/2 and beyond. Hence our results show that constancy of energy flux is not a

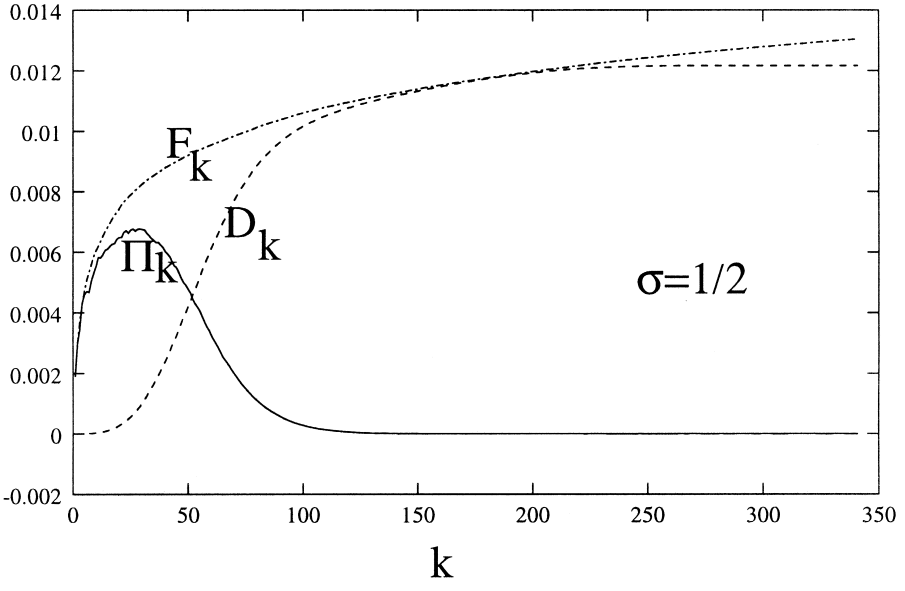

Fig. 12. The dissipation rate D_K, the energy flux Π_K, and the forcing rates F_K vs. K for $\sigma = 1/2$.

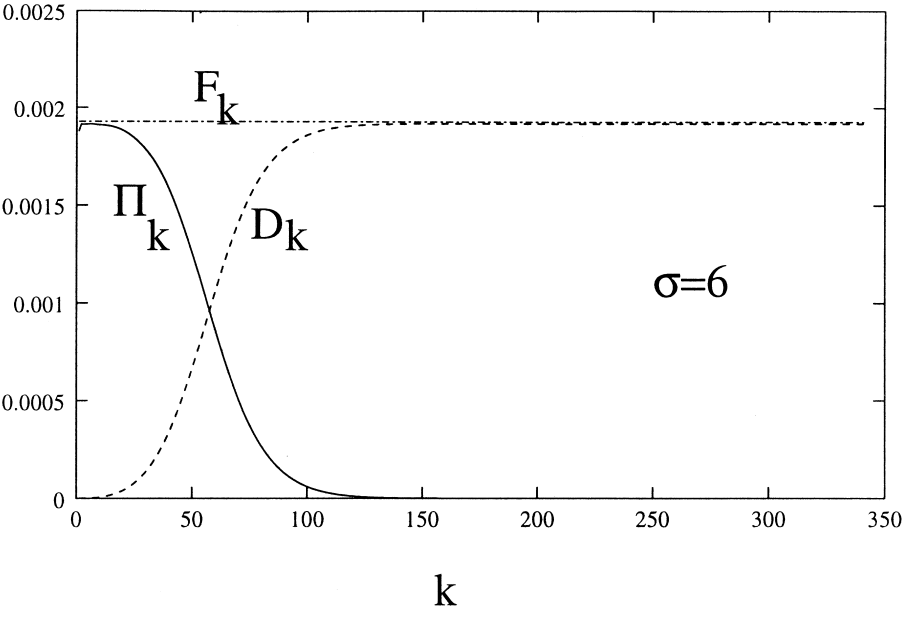

Fig. 13. The dissipation rate D_K, the energy flux Π_K, and the forcing rates F_K vs. K for $\sigma = 6$.

sufficient condition for the Kolmogorov's energy spectrum in noisy Burger equation. This indicates that the Chekhlov and Yakhot [1] argument that the constant energy cascade rate for $\sigma = 1/2$ implies Kolmogorov's energy spectrum is incomplete.

We find that for $\sigma \geqslant 2$, the flux rate $\Pi_K \approx 2\times 10^{-3}$. This numerical value is consistent with value obtained using the formula derived by Saffman [28]

$$\Pi_K \approx \frac{\mu^3}{24L}\,, \tag{7.6}$$

where μ is the velocity jump across the shock. In our simulations, $\mu \approx 0.3$ for large σ. Also, Eq. (7.4) yields the same numerical value ($2D = 2 \times 10^{-3}$).

8. Discussion and conclusions

In this paper we have numerically calculated the energy spectrum, structure function, and probability densities $(P(h), P(u), P(u'))$ for the KPZ and Burgers equations in the presence of correlated noise. The Burgers equation with a strong correlated noise ($\sigma \geqslant 3/2$) has distinct shock structures. Given this we have trivially worked out the roughening exponents for this range: $\chi_{\rm Burg} = 1/2, \chi_{\rm KPZ} = 3/2$. The χ calculated from the numerical simulation matches quite well with this result. It has been theoretically shown by many researchers that $\zeta_q^{\rm Burg} \approx 1$ when shocks are present. Numerically, we find the same $\zeta_q^{\rm Burg}$ for $\sigma \geqslant 3/2$. The probability density $P(u') \propto u'^{-\alpha}$ with $\alpha = 2.5 \pm 0.3$ for negative u'; this result is in agreement with the Polyakov's theoretical predictions. However, for positive u', our results do not match with Polyakov's predictions for this range of σ. Note that our results differ from those of E and Eijnden [17] and Kraichnan [18], who obtained $\alpha = 7/2$, and Gotoh and Kraichnan [16] who argue for $\alpha = 3$.

In the σ regime $-1 \leqslant \sigma \leqslant 0$, our numerical $\chi_{\rm KPZ}$ matches with the RG predictions. The exponent $\beta_{\rm KPZ}$, however, saturates at 0.5 contrary to the RG predictions. For $0 \leqslant \sigma \leqslant 3/2$, the exponent $\chi_{\rm KPZ}$ varies smoothly from 1 to 3/2. Boldyrev's predictions appear to match with our numerical results for $0 \leqslant \sigma \leqslant 1/2$. After that there is a significant deviation. Our claims, however, are not on a very strong ground because of large uncertainties, and hence, more exhaustive simulations are needed to reach definite conclusions.

We find in our simulation that $P(u)$ is Gaussian for all σ's and also $\zeta_q^{\rm KPZ} \propto q$. Therefore, according to the convention discussed in the introduction, the signal h will be termed as non-intermittent for all σ's. Note, however, that according to the same convention, u is as intermittent for $\sigma \geqslant 1/2$. These two statements appear to be contradictory because u and h are related by $u = -\nabla h$. The apparent contradiction is quite simple to resolve. The velocity signal u, being the derivative of h, is much more singular than h because of the presence of the shocks. That is why probability density $P(u')$ is non-Gaussian (intermittent u), even though $P(u)$ is non-Gaussian (non-intermittent h). This observation cautions us to choose a right variable while investigating the system for intermittency. Note that for fluid turbulence also, $P(u)$ is Gaussian, but $P(u')$

is not, and the variables used for structure function is u (there is no corresponding h anyway).

The nonexistence of intermittency in KPZ equation will have relevance to other models of surface growth. Sneppen and Jensen [38] and Tang and Leschhorn [39] calculated the structure function in surface growth equation in presence of quenched disorder. They find no spatial multiscaling in their system; this result could be related to the conclusions described in our paper. Sneppen and Jensen [38], and Tang and Leschhorn [39] find temporal intermittency in their model. We believe temporal structure function for the noisy KPZ and Burgers equation are important and will shed further insights into the dynamics of these systems.

Krug [40] and Kundagrami et al. [41] have investigated the existence of intermittency in the surface growth model of Das Sarma and Tamborenea (DT) [42] model and found multiscaling in it. Krug, however, finds absence of multiscaling in a variation of the DT model that was tilt independent. The DT model is related to linear Lengevin equation which is not expected to show intermittency, but Krug has attempted to relate intermittency in the DT model with the existence of relevant variables of renormalization groups. The connection of Krug's result to KPZ equation is not clear to us at this stage. Also, it is not clear whether the multiscaling in the DT model is an artifact of lattice effects, or it is due to appearance of relevant of nonlinearities in the continuum equation [40]. Another important point to note is that u of fluid turbulence should probably be mapped to h', not h as done in Krug's [40] and the Kundagrami et al. [41] papers.

In the regime $0 \leqslant \sigma \leqslant 3/2$, both structures and noise coexist. Recently, Polyakov [2], Boldyrev [14,15], Gurarie and Migdal [19], E and Eijnden [17], and Kraichnan [18] have attempted to analytically solve for the spectral exponents and the probability density $P(u')$ for this regime. Many of the recent attempts are based on methods of quantum field theory. Considering the important role played by the shock structures in determination of the roughening exponents, we believe that a calculation which incorporates both structures and noise will be very useful for such problems. The roughening exponent will get contributions both from fluctuations and embedded structures (see Appendix B). However, a careful analysis is required to isolate the individual contributions. Krishnamurthy and Barma [36] have isolated a moving pattern in the surface growth phenomena in the presence of quenched disorder. Their method may be applied here to separate the fluctuations from the structures.

Bouchaud et al. [8] have calculated the structure function of the Burgers equation in higher dimensions using the connection of KPZ equation to directed polymers. They showed that $S_q(r) \propto r$. In Appendix C we argue that using the shock structures of the higher-dimensional Burgers equation, one can obtain $S_q(r) \propto r$.

In this paper we have demonstrated the usefulness of structures in calculating the dynamical exponents of the system. The role of structures in dynamics is being studied in fluid turbulence, intermittency, self-organized criticality, etc. For example, in fluid turbulence Hatakeyema and Kambe [43] have used the vortex structures to calculate the scaling exponents. Therefore, discovery of the connections between the structures,

fluctuations, and dynamics will yield interesting insights in the non-equilibrium phenomena around us.

Acknowledgements

The author thanks Mustansir Barma, Supriya Krishnamurthy, and Deepak Dhar for discussions, references, and their kind hospitality during his stay at TIFR, where part of this work was done. V. Subrahmanyam's ideas and criticisms are gratefully acknowledged. The author also thanks J.K. Bhattacharjee, Agha Afsar Ali, Prabal Maiti, S.A. Boldyrev, and S.D. Joglekar for discussions at various stages, and R.K. Ghosh for providing computer time on DEC workstation.

Appendix A. Effects of parameters v and D

The roughening exponents of KPZ equation are usually stated without reference to the range of the parameter v and D. Usually it is assumed that v is small. This is in the same spirit as in fluid turbulence. While performing our simulations with correlated noise, we, however, found interesting changeover in the behaviour of KPZ even when v was small. We describe our findings below.

As discussed in the main text, for the parameter described in Eq. (5.1), we get the exponents shown in Table 1. However, in one of the test runs we fixed v at a somewhat higher value $v = 0.05$, and chose $D = 0.001$. For these parameters we found a transition for the energy spectrum from $k^{-2\rho-2}$ to $k^{-2\rho}$ and finally to $k^{-\chi_{\rm KPZ}}$, where $\chi_{\rm KPZ}$ is given in Table 1. To understand this transition, we need to look at the energy spectrum of Edward–Wilkinson (EW) and Random deposition (RD) models.

EW equation is given by

$$\frac{\partial h(x,t)}{\partial t} = v\nabla^2 h(x,t) + f(x,t)\,. \tag{A.1}$$

The above equation can be solved easily in Fourier space, which yields

$$h(k,\omega) = \frac{f(k,\omega)}{\mathrm{i}\omega - vk^2}\,. \tag{A.2}$$

Using

$$\langle f(k,\omega) f(k',\omega')\rangle = 2D\frac{k^{-2\rho}}{\mathrm{i}(\omega-\omega')}\,, \tag{A.3}$$

we can easily show that

$$\langle h(k,t)h^*(k,t)\rangle = k^{-2\rho-2}(A + B\exp(-2vk^2t)\,. \tag{A.4}$$

Therefore, EW equation at large t yields $|h(k)|^2 \propto k^{-2\rho-2}$.

If we substitute $\nu = 0$ in the Eq. (A.1), we obtain the Random deposition (RD) model [12] which is

$$\frac{\partial h(x,t)}{\partial t} = f(x,t)\,. \tag{A.5}$$

Using a similar procedure as above, we obtain $|h(k)|^2 \propto k^{-2\rho}$ for this equation.

Now we can explain the crossover from EW to RD and then to KPZ behaviour. In the initial phase, the width $\langle h^2 \rangle$ is small, hence the viscous term dominates both noise and nonlinear term, consequently EW behaviour is seen. As time progress and the width increases, the noise term becomes dominant and RD behaviour is observed. In this regime the width increases linearly in time [12]. At a later time when the width become large enough, the nonlinear term takes over, and KPZ like behaviour is observed. This is the reason why the spectral index varies from EW to RD, and finally to KPZ regime.

Our findings regarding the crossover from EW to KPZ, etc., show that we should be careful with the choice of parameters while simulating KPZ and Burgers equations.

Appendix B. Exponents when both structures and noise are present

A surface profile $h(x)$ can be split into two parts:

$$h(x) = h_s(x) + h_f(x)\,, \tag{B.1}$$

where $h_f(x)$ denotes the fluctuation, and $h_s(x)$ denotes the the embedded structure. By definition, $\langle h_f(x) \rangle = 0$ where $\langle . \rangle$ denotes the ensemble average. Therefore, $\langle h(x) \rangle = h_s(x)$.

We can show that the width squared W^2, which is obtained by taking the spatial average, is

$$W^2 = \overline{\langle (h(x) - \bar{h})^2 \rangle} = W_s^2 + W_f^2\,. \tag{B.2}$$

Hence, W^2 is the sum of the contributions from the fluctuating part and the structure part. Similarly, the second-order structure function $T_2(r)$ is the sum of two contributions,

$$T(r) = \overline{\langle |h(x+r) - h(x)|^2 \rangle} = T_s(r) + T_f(r)\,. \tag{B.3}$$

Hence, in a profile with an embedded structure, the exponent is determined by both structure and fluctuations.

There is no structure in KPZ profile for $\sigma = -1$, hence, the roughening exponent is totally determined by the fluctuations. However, the profile for the noiseless Burgers equation has only shock structure, which determines the roughening exponent. In KPZ equation with correlated noise, especially for $0 < \sigma < 3/2$, we have both structure and fluctuations. Therefore, we will have to do a careful analysis combining both of them to obtain the roughening exponents for these cases. We expect that similar analysis have to be carried out for the surface growth profile with quenched disorder that has both structure and fluctuations.

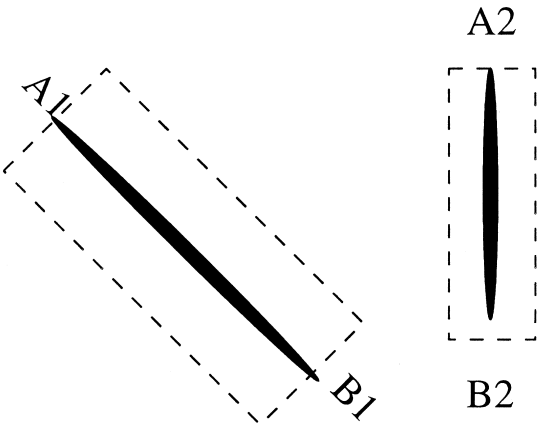

Fig. 14. The projection of shocks of two-dimensional Burgers equation. In the middle, the velocity difference across the shock is large, while at the ends A_i and B_i, the difference is small.

Appendix C. Structure function for Burgers equation in $D \geqslant 2$

The arguments of Gotoh [7] for the computation of structure function of the noiseless Burgers equation can be generalized to higher dimensions. In two dimensions the projections of the shocks will appear as shown in Fig. 14. Towards the ends (labelled as A_i and B_i in Fig. 14) the shock strength tapers off and goes to zero. The velocity in between the shocks is a smooth function, but the velocity is discontinuous at the shocks. Therefore, as argued in Section 2,

$$S_q(r) = \int |\mathbf{u}(\mathbf{x}+\mathbf{r}) - \mathbf{u}(\mathbf{x})|^q \, \mathrm{d}\mathbf{x}$$

$$\approx C_1 \frac{1}{A} \left(\frac{r}{t}\right)^q A + C_2 \frac{1}{A} \sum_i (\mu_i)^q (L_i r)\,, \tag{C.1}$$

where A is the area of the system, μ_i and L_i are the shock strength and length of the ith shock respectively, and C_1, C_2 are constants. The first term is obtained from the integral over all the space except the boxed regions near the shocks, while the second term is due to the integral in the boxed region. Essentially, we obtain $|\mathbf{u}(\mathbf{x}+\mathbf{r}) - \mathbf{u}(\mathbf{x})| \propto \mu_i$ in the boxed region when $\mathbf{x}+\mathbf{r}$ is in one side of the shock, while $\mathbf{x}$ is on the other side of the shock. This result yields $S_q(r) \propto r$ for $q > 1$. These arguments for two dimensions can be easily generalized to three and higher dimensions (in three dimensions, the shock regions will appear as disks). Hence, in any arbitrary dimensions, noiseless Burgers equation has

$$S_q(r) \propto r\,. \tag{C.2}$$

Bouchaud et al. [8] have obtained this result in D dimensions by relating to KPZ equation to directed polymer; their result becomes exact as $D \to \infty$. The strong intermittency of the Burgers equation is due to the large scale singularities of the velocity

field at the shock regions, which are concentrated in $D-1$ dimension (codimension 1). It was pointed out by one of the referee that the shocks could be fractal objects, whose fractal dimension D_f could be greater than $D-1$. The calculation of structure function for these objects is beyond the scope of this paper.

References

[1] A. Chekhlov, V. Yakhot, Phys. Rev. E 51 (1995) R1.
[2] A.M. Polyakov, Phys. Rev. E 52 (1995) 6183.
[3] F. Hayot, C. Jayaprakash, Phys. Rev. E 54 (1996) 4681.
[4] J.M. Burgers, The Nonlinear Diffusion Equation, Reidel, Boston, 1974.
[5] T. Tatsumi, S. Kida, J. Fluid Mech. 55 (1972) 659.
[6] S. Kida, J. Fluid Mech. 93 (1979) 337.
[7] T. Gotoh, Phys. Fluids A 6 (1994) 3985.
[8] J.P. Bouchaud, M. Mézard, G. Parisi, Phys. Rev. E 52 (1995) 3656.
[9] M. Kardar, G. Parisi, Y.-C. Zhang, Phys. Rev. Lett. 56 (1986) 889.
[10] E. Medina, T. Hwa, M. Kardar, Phys. Rev. A 39 (1989) 3053.
[11] A.K. Chattopadhyay, J.K. Bhattacharjee, Europhys. Lett. 42 (1998) 119.
[12] A.-L. Barabasi, H.E. Stanley, Fractal Concepts in Surface Growth, Cambridge University Press, New York, 1995.
[13] U. Frisch, Turbulence, Cambridge University Press, Cambridge, 1995.
[14] S.A. Boldrev, Phys. Rev. E 55 (1997) 6907.
[15] S.A. Boldrev, Phys. Plasmas 5 (1998) 1681.
[16] T. Gotoh, R. Kraichnan, chao-dyn/9803037, 1998.
[17] W.E. Eȳnden, E.V. Eijnden, Phys. Rev. Lett. 83 (1999) 2572.
[18] R.H. Kraichnan, chao-dyn/9901023, 1999.
[19] V. Gurarie, A. Migdal, Phys. Rev. E 54 (1996) 4908.
[20] E. Balkovsky, G. Falkovich, I. Kalokolov, V. Lebedev, Phys. Rev. Lett. 78 (1997) 1452.
[21] V. Yakhot, A. Chekhlov, Phys. Rev. Lett. 77 (1996) 3118.
[22] Y.-C. Zhang, Phys. Rev. A 42 (1990) 4897.
[23] H.G.E. Hentschel, F. Family, Phys. Rev. Lett. 66 (1991) 1982.
[24] C.-K. Peng, S. Havlin, M. Schwartz, H.E. Stanley, Phys. Rev. A 44 (1991) R2239.
[25] J.G. Amar, P.-M. Lam, F. Family, Phys. Rev. A 43 (1991) 4548.
[26] P. Meakin, R. Jullien, Europhys. Lett. 9 (1989) 71.
[27] P. Meakin, R. Jullien, Phys. Rev. A 41 (1990) 983.
[28] P.G. Saffman, in: N.J. Zabusky (Ed.), Topics in Nonlinear Physics, Springer, Berlin, 1968, pp. 485–614.
[29] C. Maneveau, K.R. Sreenivasan, Phys. Rev. Lett. 59 (1987) 1424.
[30] C. Meneveau, K.R. Sreenivasan, in: M.-D. Van, B. Nichols (Eds.), Physics of Chaos and Systems far from Equilibrium, North-Holland, Amsterdam, 1987, pp. 47–76.
[31] M.J. Lighthill, Introduction to Fourier Analysis and Generalised Functions, Cambridge University Press, Cambridge, 1959.
[32] C. Canuto, M.Y. Hussaini, A. Quarteroni, T.A. Zhang, Spectral Methods in Fluid Turbulence, Springer, Berlin, 1988.
[33] K. Moser, J. Kertész, D.E. Wolf, Physica A 178 (1991) 215.
[34] M.K. Verma, D.A. Roberts, M.L. Golstein, S. Ghosh, W.T. Stribling, J. Geophys. Res. 101 (1996) 21 619.
[35] W.H. Press, B.P. Flannery, S.A. Teukolsky, W.T. Vetterling, Numerical Recipes in C, 2nd Edition, Cambridge University Press, Cambridge, 1992.
[36] S. Krishnamurthy, M. Barma, Phys. Rev. Lett. 76 (1996) 423.
[37] W.D. McComb, The Physics of Fluid Turbulence, Clarendon Press, Oxford, 1990.
[38] K. Sneppen, M.H. Jensen, Phys. Rev. Lett. 71 (1993) 101.
[39] L.-H. Tang, H. Leschhorn, Phys. Rev. A 45 (1992) R8309.

[40] J. Krug, Phys. Rev. Lett. 72 (1994) 2907.
[41] A. Kundagrami, C. Dasgupta, P. Punyindu, S.D. Sarma, chao-dyn/9901023, 1999.
[42] S.D. Sarma, P. Tamborenea, Phys. Rev. Lett. 66 (1991) 325.
[43] N. Hatakeyama, T. Kambe, Phys. Rev. Lett. 79 (1997) 1257.